THE JOURNAL OF BIOLOGICAL CHEMISTRY VOL. 285, NO. 33, pp. 25859–25866, August 13, 2010

SENP1 Induces Prostatic Intraepithelial Neoplasia through Multiple Mechanisms*[S]

Received for publication, April 16, 2010, and in revised form, June 10, 2010 Published, JBC Papers in Press, June 15, 2010, DOI 10.1074/jbc.M110.134874

Tasneem Bawa-Khalfe[‡1], Jinke Cheng[‡§], Sue-Hwa Lin[¶], Michael M. Ittmann[‖], and Edward T. H. Yeh[‡2]**

*From the Departments of [‡]Cardiology and [¶]Molecular Pathology, The University of Texas MD Anderson Cancer Center, the [‖]Department of Pathology, Baylor College of Medicine, and the **Texas Heart Institute/St. Luke's Episcopal Hospital, Houston, Texas 77030 and the [§]Departments of Biochemistry and Molecular & Cell Biology, The Key Laboratory of Cell Differentiation and Apoptosis of Chinese Ministry of Education, Shanghai Jiao Tong University School of Medicine, Shanghai 200025, China*

SUMOylation has been shown to modulate DNA replication/repair, cell cycle progression, signal transduction, and the hypoxic response. SUMO (small ubiquitin-like modifier)-specific proteases regulate SUMOylation, but how changes in the expression of these proteases contribute to physiological and/or pathophysiological events remains undefined. Here, we show that SENP1 (sentrin/SUMO-specific protease 1) is highly expressed in human prostate cancer specimens and correlates with hypoxia-inducing factor 1α (HIF1α) expression. Mechanistic studies in a mouse model indicate that androgen-driven expression of murine SENP1 leads to HIF1α stabilization, enhanced vascular endothelial growth factor production, and angiogenesis. Further pathological assessment of the mouse indicates that SENP1 overexpression induces transformation of the normal prostate gland and gradually facilitates the onset of high-grade prostatic intraepithelial neoplasia. Consistent with cell culture studies, SENP1 enhances prostate epithelial cell proliferation via modulating the androgen receptor and cyclin D_1. These results demonstrate that deSUMOylation plays a critical role in prostate pathogenesis through induction of HIF1α-dependent angiogenesis and enhanced cell proliferation.

SUMO (small ubiquitin-like modifier) modification of protein substrates is a dynamic process that modulates the target protein's expression, function, and/or subcellular location (1, 2). SUMOylation is regulated by SUMO-specific activating (E1), conjugating (E2), and ligating (E3) enzymes and reversed by a family of sentrin/SUMO-specific proteases (3–5). These enzymes are critical for maintaining a balance between the level of SUMOylated and unmodified cellular substrates and hence play an important role in mediating normal cellular physiology.

Several large-scale gene expression studies report changes in the levels of SUMO E1, E2, and *SENP1* (sentrin/SUMO-specific protease 1) in various cancers, suggesting an imbalance in the SUMO system (6–9). *SENP1* mRNA levels are elevated in thyroid oncocytic adenocarcinoma (6) and human prostate cancer (PCa)[3] (10). In addition, using *in situ* hybridization, we recently found greater *SENP1* mRNA levels in precancerous prostatic intraepithelial neoplasia (PIN) compared with adjacent normal prostate epithelia (10). Transformation of the normal prostate epithelia to carcinoma is preceded by the development of this well characterized PIN state (11). The presence of elevated *SENP1* levels in this precursor state posed the question as to whether SENP1 induction is not associated merely with the carcinoma but instead could directly contribute to prostate carcinogenesis.

Recently, we demonstrated that SENP1 enhances the stability of hypoxia-inducing factor 1α (HIF1α) and, consequently, HIF1α-mediated transcription; in the absence of SENP1, HIF1α is actively SUMOylated and subsequently degraded under hypoxic conditions (12). In prostate carcinogenesis, hypoxic tissue environments emerge due to rapidly proliferating cancer cells, and HIF1α is postulated to modulate the expression of genes required either to enhance oxygen availability or to adapt metabolically to the decreased oxygen environment (13, 14). To promote the former, HIF1α increases the transcription of the vascular endothelial growth factor (VEGF), which in turn induces formation of the neovasculature or angiogenesis. Angiogenesis is critical to facilitate cancer cell growth, and therefore, HIF1α and the HIF1α-regulated VEGF are essential to initiate the switch in the cancer environment from anti-angiogenic to pro-angiogenic. We reported that SENP1 alters VEGF levels by directly regulating HIF1α stability during fetal development (12), but it is unknown whether SENP1 promotes angiogenesis via regulation of HIF1α in adult mice.

In this study, we found that SENP1 levels correlate with HIF1α in human prostate carcinoma. SENP1 expression correlates with the severity of the disease, as high levels of SENP1 are observed in more aggressive PCa. To evaluate the contribution of SENP1 to PCa development, we generated transgenic mice

* This work was also supported, in whole or in part, by National Institutes of Health Grants CA139520 (to E. T. H. Y.), P50CA058204 (to the Baylor Prostate Cancer SPORE, M. M. I.), and CA111479 (to S.-H. L.) from NCI. This work was also supported by United States Department of Defense Grants PC040121 (to E. T. H. Y.) and PC060932 (to J. C.) and the Prostate Cancer Development Award from The University of Texas MD Anderson Cancer Center (to E. T. H. Y.).

[S] The on-line version of this article (available at http://www.jbc.org) contains supplemental Figs. 1 and 2.

[1] Supported in part by National Research Service Award F32-CA110620 from the National Institutes of Health.

[2] To whom correspondence should be addressed: Dept. of Cardiology, The University of Texas MD Anderson Cancer Center, Unit 449,1515 Holcombe Blvd., Houston, TX 77030. Tel.: 713-792-6242; Fax: 713-745-1942; E-mail: etyeh@mdanderson.org.

[3] The abbreviations used are: PCa, prostate cancer; PIN, prostatic intraepithelial neoplasia; HIF1α, hypoxia-inducing factor 1α; VEGF, vascular endothelial growth factor; AR, androgen receptor; PCNA, proliferating cell nuclear antigen; PECAM, platelet endothelial cell adhesion molecule.

with an androgen-driven murine *Senp1* transgene overexpressed in the prostate gland. SENP1 transgenic mice exhibited increased expression of HIF1α with progression of the dysplasia. The enhanced HIF1α stability in the SENP1 transgenic mice produced elevated VEGF expression. Consequently, it is not surprising that angiogenesis was readily observed in these SENP1 transgenic mice compared with age-matched wild-type mice. We have reported previously our initial histological studies on two 4-month-old founder mice that showed the presence of hyperplasia in the dorsolateral lobe of the prostate compared with age-matched wild-type mice (10). In this study, we demonstrate in two lines of SENP1 transgenic mice that the hyperplasia further progresses to develop PIN. Also, high-grade PIN was observed in the transgenic mice line with the greater level of the *Senp1* transgene. Enhanced proliferation of prostate epithelia was observed in the SENP1-overexpressing mice, and concurrently, pro-oncogenic factors, specifically the androgen receptor (AR) and cyclin D_1, were elevated. Thus, SENP1 participates in the development of prostate neoplasia.

EXPERIMENTAL PROCEDURES

Plasmids and Antibodies—The FLAG-SENP1 and FLAG-SENP1(C603A) plasmids have been described previously (15, 16) and were prepared by standard cloning methods and PCR-based mutagenesis. The cyclin D_1 promoter region (−1745/+134) was inserted into the luciferase reporter vector as described in a previous protocol (17, 18). The primers used were those for the cyclin D_1 promoter (−1745/+134): 5′-CAGCTGGGCCGCCCTTGT-3′ (sense) and 5′-CAGCTGGGGAGGGCTGTGG-3′ (antisense).[4] We used antibodies against FLAG (M2) and actin (Sigma), cyclin D_1 (Pharmingen), Ki67 (Novocastra, Newcastle upon Tyne, UK), proliferating cell nuclear antigen (PCNA) and VEGF (Santa Cruz Biotechnology, Santa Cruz, CA), SENP1 (Invitrogen), HIF1α (Novus Biologicals, Littleton, CO), and CD31/PECAM (BD Biosciences). The anti-AR antibody was kindly provided by Dr. Zhengxin Wang (The University of Texas MD Anderson Cancer Center).

RNA Isolation and Quantitative Reverse Transcription-PCR—Cells were prepared for RNA isolation using the TRIzol reagent (Invitrogen) according to manufacturer's instructions with stock samples diluted to the appropriate concentrations with diethyl pyrocarbonate-treated water. Quantitative reverse transcription-PCR was conducted with the OneStep reverse transcription-PCR kit from Qiagen (Valencia, CA) to illustrate differences in *Senp1* transgene levels with respect to the housekeeping gene *G3PDH*. The following primers were used for amplification of the *Senp1* transgene or *G3PDH* mRNA: *Senp1* transgene, 5′-GACGACAAGCTTGCGGCC-3′ (forward) and 5′-GGGCTTAAAAGACTCCGACGA-3′ (reverse); and *G3PDH*, 5′-AACTTTGGCATTGTGGAAGGGCTC-3′ (forward) and 5′-TGGAAGAGTGGGAGTTGCTGTTGA-3′ (reverse).

Generation of the Senp1 Transgene—A murine SENP1 transgenic vector was constructed by ligating the gene fragments to the pBluescript SK(+) backbone (Stratagene, La Jolla, CA). The 5′-flanking promoter region (−244/−96 + −286/+28) of the rat probasin gene was subcloned into the SacI and NotI sites located in multiple cloning site. The hemagglutinin-FLAG-tagged murine *Senp1* cDNA was subcloned into the NotI and SalI sites of the SK(+) backbone. The poly(A) tail of human growth hormone was subcloned into the SalI and ApaI sites of the SK(+) multiple cloning site.

The construct was sequenced, and we found that transient transfection of the probasin promoter was inducible by the synthetic androgen R1881 in LNCaP cells. Activation of the promoter by R1881 also prompted induction of hemagglutinin-FLAG-tagged murine SENP1, and this SENP1 induction was sufficient to enhance AR-dependent transcription (data not shown). Therefore, the construct was both inducible and biologically active.

Isolation and Preparation of Tissue—The genitourinary bloc was isolated, and the four lobes of the mouse prostate were microdissected with the aid of a dissecting microscope. The tissue was fixed overnight with 10% buffered formalin, dehydrated with 70% ethanol, and embedded in paraffin. The embedded tissue was cut into 5-μm sections and placed on slides.

For assessment of human PCa, we obtained slides that included 17 radial prostatectomy samples, which had been evaluated previously by a pathologist. The slides included carcinomas with Gleason grades of 3, 4, and/or 5. Specifically, 10 samples included a primary or secondary grade of 3, eight samples expressed grade 4 carcinomas, and in four samples included grade 5 carcinomas.

Hematoxylin/Eosin Staining and Immunohistochemistry—The slides were rehydrated gradually with ethanol, stained with hematoxylin for 3 min and eosin for an additional 3 min, dehydrated through an ethanol gradient, incubated in xylene, and covered with a coverslip. For immunohistochemical analysis, the samples were first rehydrated and then exposed to two antigen retrieval steps. First, the slides were placed in boiling citrate buffer (pH 6.4) for 30 min and subsequently treated with proteinase K (20 μg/ml) at room temperature for 10 min. Endogenous peroxides were then quenched with 3% hydrogen peroxide treatment for 10 min at room temperature. The slides were placed in blocking serum for 30 min and incubated overnight with the primary antibody in a humidified chamber. The slides were washed three times in phosphate-buffered saline and exposed to the appropriate secondary antibody for 1 h in a humidified chamber. After three washes in phosphate-buffered saline, the slides were placed in ABC reagent (Vector Laboratories, Burlingame, CA) for 1 h in a humidified chamber, washed three times in phosphate-buffered saline, and then incubated with the diaminobenzidine solution (Vector Laboratories) for 2–10 min at room temperature. The diaminobenzidine reaction was terminated by placing the slides in distilled H_2O. Some slides were counterstained with hematoxylin for 1 min prior to dehydration gradually with ethanol.

Protein Extraction from Prostate Tissue and Western Blot Analysis—Frozen microdissected prostate gland tissue was incubated in radioimmune precipitation assay buffer (Cell Signaling, Danvers, MA) with protease inhibitor mixture (Sigma) for 30 min with agitation at 4 °C. The tissue samples were homogenized and subsequently sonicated. Protein concentrations in the samples were calculated with the BCA protein assay

[4] Details of the construction of the plasmids are available upon request.

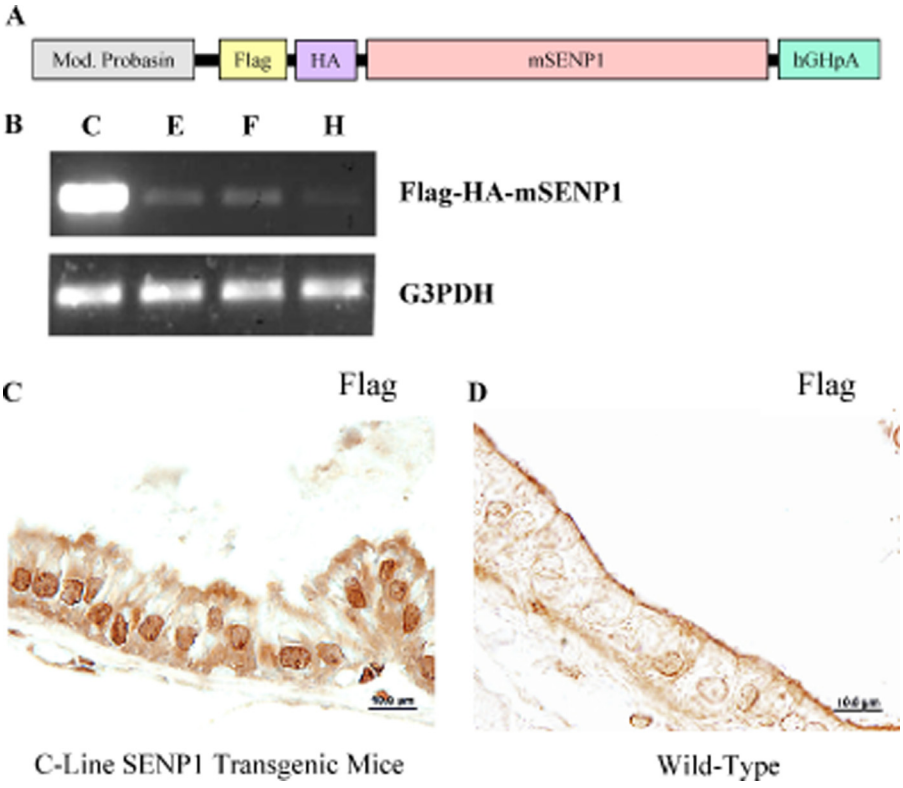

FIGURE 1. ***Senp1* transgene expression in mouse prostate.** *A*, shown is a schematic representation of the *Senp1* transgene described in detail under "Experimental Procedures." *Mod. Probasin*, modified probasin promoter; *HA*, hemagglutinin; *mSENP1*, mouse SENP1; *hGHpA*, human growth hormone poly(A). *B*, four transgenic mice lines with the probasin-driven *Senp1* transgene were identified using specific PCR primers. Varying levels of the *Senp1* transgene were expressed; the E-, F-, and H-line mice expressed lower levels of the *Senp1* transgene in comparison with the C-line mice. *G3PDH*, glyceraldehyde-3-phosphate dehydrogenase. *C* and *D*, prostate tissue sections (5 μm) from C-line transgenic and wild-type mice, respectively, were incubated with a primary anti-FLAG antibody and detected using a diaminobenzidine kit.

(Thermo Scientific, Rockford, IL) according to manufacturer's protocol. 30 μg of protein extract was subjected to Western blot analysis as described previously (18).

Data Analysis—Student's *t* test analysis was conducted with GraphPad Prism Version 4.0 (GraphPad Software, La Jolla, CA). The log rank test was used to compare the Kaplan-Meier survival curves for the incidence of lesions (both hyperplastic and neoplastic) in the dorsolateral lobes of wild-type *versus* SENP1 transgenic mice. The difference between groups was considered statistically significant when the p value was <0.05.

RESULTS

Senp1 Transgene Expression in the Prostate Gland—Previously, we demonstrated that agonist-occupied AR directly binds the *SENP1* promoter and subsequently induces SENP1 expression (19). To closely mimic this endogenous regulation of SENP1 expression, we generated a transgenic mouse in which the *Senp1* transgene was driven via the androgen-regulated probasin promoter (Fig. 1*A*). Hence, SENP1 is overexpressed in the prostate gland after puberty. In a preliminary report, we showed data from two founder transgenic mice that exhibited hyperplasia at 4 months of age (10). The founder mice were bred with wild-type mice to establish germ lines. RNA isolated from prostate tissue helped identify four lines with varying levels of the *Senp1* transgene (Fig. 1*B*); the E-, F-, and H-line mice expressed lower levels of the *Senp1* transgene in comparison with the C-line mice. Cellular distribution of the SENP1 protein was assessed by immunostaining with an antibody directed against the FLAG tag of the *Senp1* (Fig. 1*A*). The immunohistochemical analysis illustrated the expression of the SENP1 protein predominantly in the nuclei of the epithelial cells of 4-month-old C-line transgenic mice (Fig. 1*C*). In contrast, tissue from age-matched wild-type mice did not exhibit any specific staining with the anti-FLAG antibody (Fig. 1*D*).

Overexpression of SENP1 in Mouse Prostate Tissue Induces PIN—Histological studies presented clear structural differences in the dorsolateral lobes isolated from these 4-month-old C-line transgenic mice (Fig. 2, *A* and *B*, ×20 and ×60 magnification, respectively) relative to age-matched wild-type mice (Fig. 2, *C* and *D*, ×20 and ×60 magnification, respectively). Normal prostate glands isolated from wild-type mice included a flat monolayer of epithelial cells (Fig. 2, *C* and *D*, *white arrow*) that line a large central lumen (Fig. 2*C*). In contrast, the C-line transgenic mice exhibited multiple layers of prostate epithelial cells with formation of papillae and distinct nuclear atypia. The nuclei of the atypical cells were hyperchromatic and enlarged (Fig. 2*B*, *black arrow*) in comparison with the small round nuclei of normal adjacent epithelial cells (Fig. 2*D*, *white arrow*). Six additional C-line mice of the same age were assessed and displayed similar atypical epithelial cells; however, some mice exhibited a greater population of atypical cells than others. We identified these abnormalities as signs of stage I or low-grade PIN. Hence, the results suggested that the onset of PIN in C-line transgenic mice was as early as 4 months.

Subsequently, prostate tissue was isolated from 6-, 8-, 10-, and 12-month-old C-line mice. A greater population of atypical epithelial cells in the dorsolateral prostates of older C-line transgenic mice (Fig. 2, *E*, *F*, *I*, and *J*, and supplemental Fig. 1) is observed as compared with either the 4-month-old C-line mice (Fig. 2, *A* and *B*) or the respective age-matched wild-type control mice (Fig. 2, *G*, *H*, *K*, and *L*, and supplemental Fig. 1). The prostate gland of the 8-month-old C-line transgenic mouse illustrated stage II PIN; specifically, the epithelial cells had a loss of uniformity and were invading the lumen (Fig. 2, *E* and *F*). Prostate tissue from 12-month-old C-line mice showed stage IV or high-grade PIN. The abnormal epithelial cells encompassed the majority of the central lumen, the enlarged stroma appeared to surround the gland, and signs of an inflammatory response were evident with the enhanced appearance of macro-

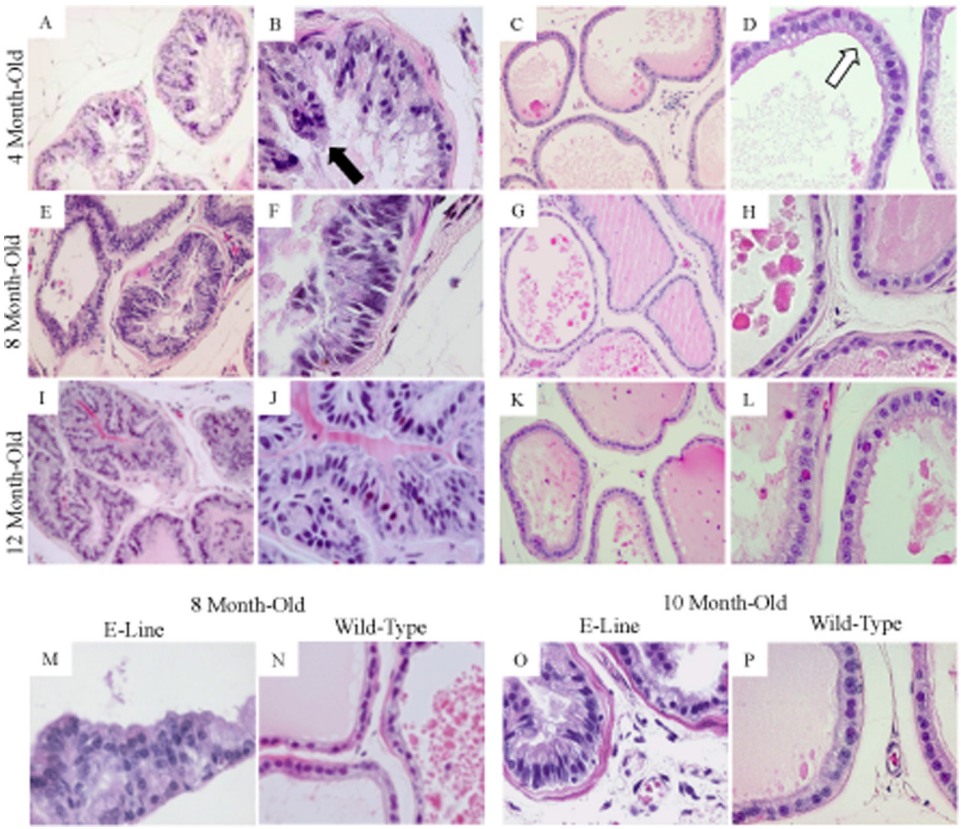

FIGURE 2. **SENP1 expression determines onset of PIN.** The prostates were assessed in the high *Senp1* transgene-expressing C-line mice *versus* age-matched wild-type mice at 4 months (*A*/*B* and *C*/*D*, respectively), 8 months (*E*/*F* and *G*/*H*, respectively), and 12 months (*I*/*J* and *K*/*L*, respectively) of age. Samples were hematoxylin/eosin-stained and evaluated at ×20 (*A*, *C*, *E*, *G*, *I*, and *K*) and ×60 (*B*, *D*, *F*, *H*, *J*, and *L*) magnification. The *white arrow* indicates normal epithelial cells, whereas the *black arrow* identifies abnormal nuclei. Hyperplasia was observed at 8 month of age (*M*) in the low *Senp1* transgene expresser (E-line), and low-grade PIN was readily present at 10 months of age (*O*) as compared with age-matched wild-type mice (*N* and *P*, respectively).

phages in several additional prostate samples (Fig. 2, *I* and *J*). Therefore, the C-line transgenic mice exhibited significantly greater incidence of hyperplastic and neoplastic lesions in the dorsolateral lobe with increases in age compared with their age-matched wild-type counterparts (log rank test, $p < 0.001$). As opposed to the dorsolateral lobe, the anterior and ventral lobes did not show any significant changes possibly due to lesser expression of the *Senp1* transgene in these two lobes as observed via immunohistochemical analysis with the anti-SENP1 antibody. C-line SENP1 transgenic mice did not develop carcinoma even when assessed at 16 months of age ($n = 6$).

Aberrant prostate epithelial cells were also observed in the dorsolateral lobes of low *Senp1* transgene-expressing E-line mice. 8-Month-old E-line SENP1 transgenic mice (Fig. 2*M*) exhibited signs of hyperplasia. In the prostate sample (Fig. 2*M*), the epithelial cells lost their monolayer formation but maintained small round nuclei, which were distinct from the nuclei of epithelial cells from either 4-month-old C-line transgenic mice (Fig. 2, *A* and *B*) or 8-month-old wild-type mice (Fig. 2*N*). The onset of PIN I or low-grade PIN occurred at 10 months of age in the E-line mice. The nuclei of atypical cells in 10-month-old E-line mice ($n = 4$) (Fig. 2*O*) closely resembled cell nuclei in 4-month-old C-line mice (Fig. 2*B*) but not the 10-month-old wild-type mice (Fig. 2*P*). Therefore, comparison of the high and low *Senp1* transgene-expressing mice (C- and E-lines, respectively) suggests that the level of SENP1 in the prostate dictates the time of PIN onset; if the SENP1 levels are high, then PIN will be observed at an earlier age.

SENP1 Regulates Prostate Cell Proliferation—To evaluate changes in epithelial cell proliferation, PCNA immunostaining was conducted on tissue samples. Prostate epithelia from the PIN-expressing 4-month-old C-line transgenic mice (Fig. 3*A*) exhibited high levels of PCNA staining compared with the age-matched wild-type mice (Fig. 3*B*). The number of nuclei that stained positive for PCNA was consistently greater in tissue samples from the 4-month-old C-line transgenic compared with the age-matched wild-type mice (Fig. 3*C*), as assessment of three additional 4-month-old C-line mice and two wild-type mice provided similar results. Immunostaining for an additional proliferation maker, specifically Ki67, provided similar results (data not shown). Collectively, these results indicated an increase in epithelial cell proliferation of 4-month-old C-line mice exhibiting low-grade PIN. These observations in the SENP1 transgenic mouse model are consistent with our previous results that demonstrated the ability of SENP1 to modulate prostate epithelial cell proliferation (19).

Our previous studies established an interdependent relationship between SENP1 and AR (10, 18, 19), and it is known that enhanced AR expression facilitates growth of prostate epithelial cells (20). Hence, we investigated the level of AR in the prostate glands of mice with elevated SENP1 levels. As expected, expression of the *Senp1* transgene caused significantly greater total SENP1 protein levels in prostate glands isolated from 4-month-old C-line SENP1 transgenic mice compared with age-matched wild-type mice (Fig. 3*D*). Interestingly, this induction of SENP1 was accompanied by an increase in AR in this prostate sample (Fig. 3*D*) and in additional samples from 4-month-old SENP1 transgenic mice. In addition, elevated SENP1 also prompted enhanced expression of the key cell cycle regulator cyclin D_1 (Fig. 3*D*). Previous results from our laboratory demonstrated that the catalytic activity of SENP1 facilitates cyclin D_1 expression in the AR-positive and AR-negative prostate cancer cell lines LNCaP and PC-3, respectively (10). Additional mechanistic studies in SENP1-overexpressing LNCaP cells indicated that SENP1 does not affect cyclin D_1 protein stability but instead directly regulates transcription of the cyclin D_1 gene (supplemental Fig. 2, *A* and *B*).

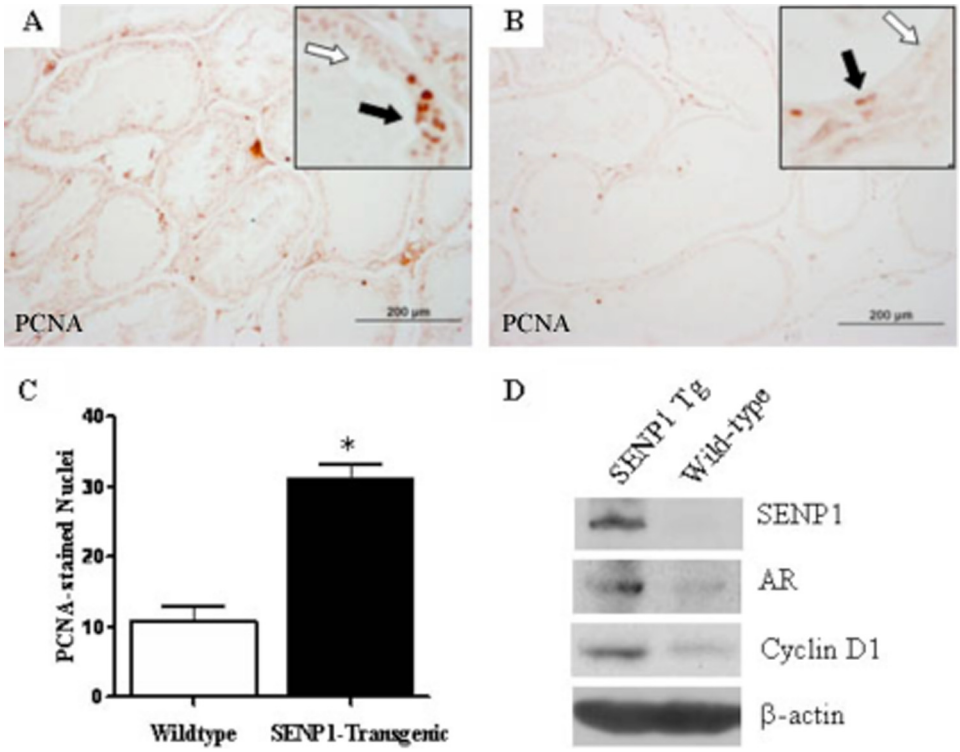

FIGURE 3. **SENP1 enhances prostate epithelial cell proliferation via modulating expression of critical oncogenes.** *A* and *B*, prostate tissue sections (5 μm) were incubated with primary anti-PCNA antibody and detected using a diaminobenzidine kit. *C*, PCNA-positive nuclei were counted in three randomly selected fields at ×40 magnification for each of the 4-month-old C-line mouse samples (representative of three independent studies). Student's *t* test was used to evaluate differences between the groups. *, $p < 0.05$. *D*, prostate tissue was microdissected from 4-month-old C-line SENP1 transgenic (*Tg*) and wild-type mice. 30 μg of each prepared prostate protein sample was assayed for expression of SENP1, AR, cyclin D_1, and the loading control β-actin with specific antibodies.

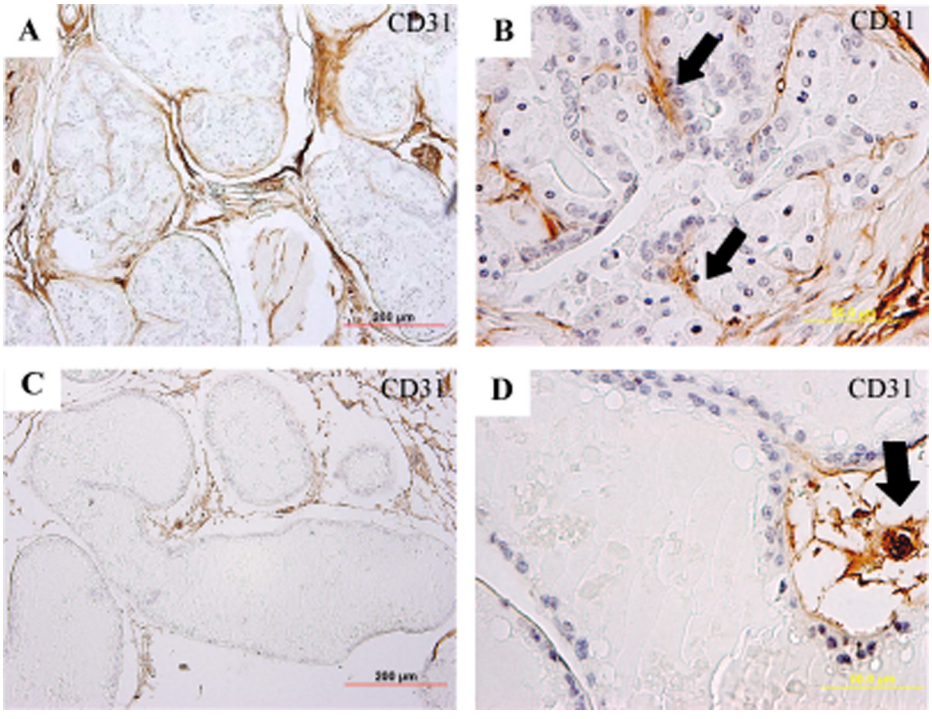

FIGURE 4. **Prostate glands of SENP1 transgenic mice exhibit signs of angiogenesis.** Prostate tissue from 12-month-old C-line SENP1 transgenic (*A* and *B*) and wild-type (*C* and *D*) mice was stained with anti-CD31/PECAM antibody to evaluate the vascular bed and counterstained with hematoxylin. SENP1 transgenic mice appeared to express a greater number of intraductal capillaries adjacent to the epithelial cells (*A* and *B*) than age-matched wild-type mice (*C* and *D*).

SENP1 Transgenic Mice Enhance Angiogenesis via Stabilization of HIF1α—The anti-CD31/PECAM antibody indicated a clear difference in the vascular architecture in the prostates of 12-month-old C-line transgenic mice (Fig. 4, *A* and *B*) *versus* age-matched wild-type mice (Fig. 4, *C* and *D*). There was a clear increased density of capillaries adjacent to epithelial cells in prostate tissue samples from transgenic mice (Fig. 4, *A* and *B*) compared with wild-type mice (Fig. 4, *C* and *D*). Normal prostate glands expressed interductal vascular beds (Fig. 4, *C* and *D*), but in the SENP1 transgenic mice, neovasculature was evident within the lumen of the gland (Fig. 4*B*, *black arrows*). Hence, 12-month-old C-line transgenic mice, which exhibited high-grade PIN but no carcinoma (Fig. 2, *I* and *J*), did show clear signs of angiogenesis.

HIF1α is a known mediator of angiogenesis. Recently, we demonstrated that knock-out of SENP1 in mice leads to ubiquitin-dependent degradation of HIF1α under hypoxic conditions; hence, SENP1 regulates HIF1α stability during development (12). However, it is unknown whether SENP1 also regulates HIF1α in adult tissue. Here, we postulated that HIF1α levels would be significantly elevated in the SENP1-overexpressing transgenic mice. The 4-month-old C-line transgenic mice that expressed high levels of the SENP1 protein in the nucleus (Fig. 1*C*) also exhibited an elevation of HIF1α in the nuclei of epithelial cells from the dorsolateral lobe of the prostate (Fig. 5*A*). In contrast, prostate tissue from 4-month-old wild-type mice did not express detectable HIF1α protein levels (Fig. 5*B*). Elevated HIF1α levels were also increased in 12-month-old C-line SENP1 transgenic mice compared with the respective age-matched wild-type mice (Fig. 5, *C* and *D*). Analysis of additional mice at 4 and 12 months of age confirmed that the transcriptional active forms of HIF1α (HIF1α in the nucleus) were significantly

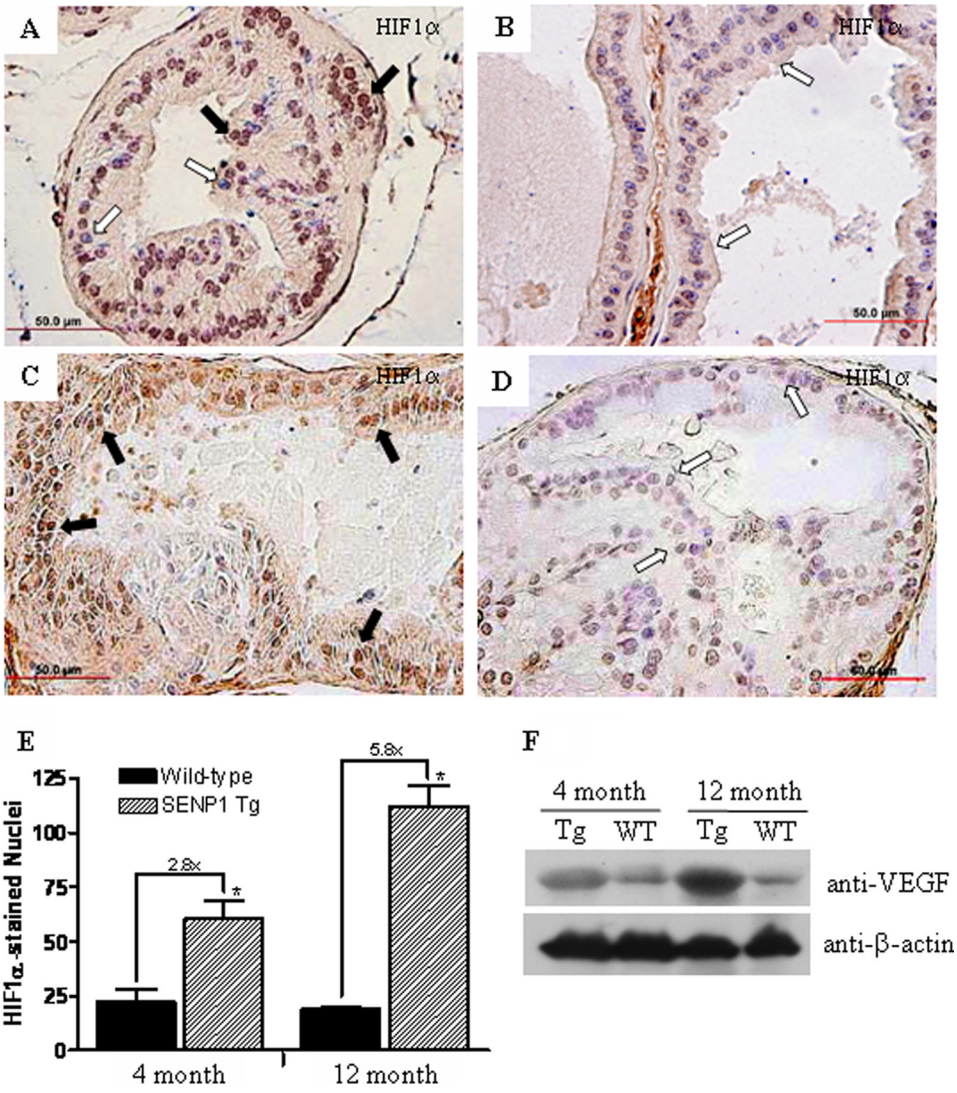

FIGURE 5. **Protein levels of HIF1α and HIF1α-regulated VEGF are elevated in SENP1 transgenic mice.** HIF1α expression was assessed in the sectioned prostate tissue from C-line SENP1 transgenic and wild-type mice that were 4 (*A* and *B*, respectively) and 12 (*C* and *D*, respectively) months old. *E*, the number of nuclei that stained positive for HIF1α was determined under ×40 magnification for samples from three different C-line transgenic and age-matched wild-type mice. The *black arrows* in *A* and *C* indicate HIF1α-positive nuclei, whereas the *white arrows* indicate HIF1α-negative nuclei. Student's *t* test was used to evaluate differences between the groups. *, $p < 0.05$. *F*, prostate protein samples from SENP1 transgenic (*Tg*) and wild-type (*WT*) mice 4 and 12 months of age were assessed for VEGF levels, whereas β-actin served as a loading control.

greater in the SENP1 transgenic mice than in the wild-type mice (Fig. 5*E*). Thus, HIF1α levels were significantly elevated in the SENP1-overexpressing transgenic mice.

We further analyzed the levels of VEGF, a downstream target gene of HIF1α that contributes to the HIF1α-driven angiogenic response. VEGF levels were significantly greater in the prostate glands of both 4- and 12-month-old SENP1 transgenic mice compared with prostate tissue isolated from age-matched wild-type mice (Fig. 5*F*). Similar results were obtained with immunohistochemical analysis, as greater cytosolic expression of the VEGF protein was readily detectable in prostate tissue from 12-month-old SENP1 transgenic mice (data not shown).

Correlation between SENP1 and HIF1α in Human Prostate Cancer—Elevated HIF1α levels are commonly observed in human PCa and are associated with more aggressive forms of the carcinoma (14, 21, 22). Because our previous studies suggested that SENP1 stabilizes HIF1α in mouse embryonic fibroblast cells and the studies above presented a similar phenomenon in adult mice, we sought to determine whether the level of SENP1 correlates with the elevated levels of HIF1α in human PCa. Gleason grade 3, 4, and 5 carcinomas were assessed following immunostaining with the anti-SENP1 antibody (Fig. 6, *A–C*, respectively). Several nuclei stained positive for SENP1 (Fig. 6, *A–C*, *black arrows*) and could be distinguished from the nuclei that did not express the SENP1 protein via the hematoxylin counterstain (Fig. 6, *A–C*, *white arrows*). Hence, we could readily count the number of SENP1-positive nuclei *versus* the total number of nuclei (brown SENP1-stained and blue/purple hematoxylin-stained) under ×40 magnification. This assessment indicated that the number of nuclei positive for SENP1 was significantly greater in grade 4 and 5 carcinomas than in grade 3 carcinomas (Fig. 6*G*); hence, up-regulation of SENP1 protein levels corresponds to PCa aggressiveness. In this study, nuclear expression of HIF1α was greater in the samples from patients with higher Gleason grades (Fig. 6, *D–F*, *black arrows*); this observation is in accord with previous reports (23, 24). The increase in the nuclear expression of HIF1α accompanied the elevation of SENP1 levels in each PCa grade (Fig. 6*G*).

DISCUSSION

Analysis of *in situ* hybridization studies in our previous work suggested elevated levels of *SENP1* message in human PIN lesions and PCa specimens (10). We now report that up-regulation of SENP1 protein directly correlated with aggressive PCa (Fig. 6). Hence, in human PCa, induction of SENP1 occurs early with the development of precancerous neoplastic lesions and manifests with onset of aggressive carcinoma. To evaluate the contribution of SENP1 to prostate carcinogenesis, the SENP1 transgenic mouse model was generated. In this study, we have demonstrated that increasing SENP1 in the mouse prostate actively induces transformation of the normal gland via facilitating pro-growth and angiogenic pathways (Fig. 7).

Our collective body of work in human PCa cells indicates that SENP1 overexpression can regulate various growth/pro-

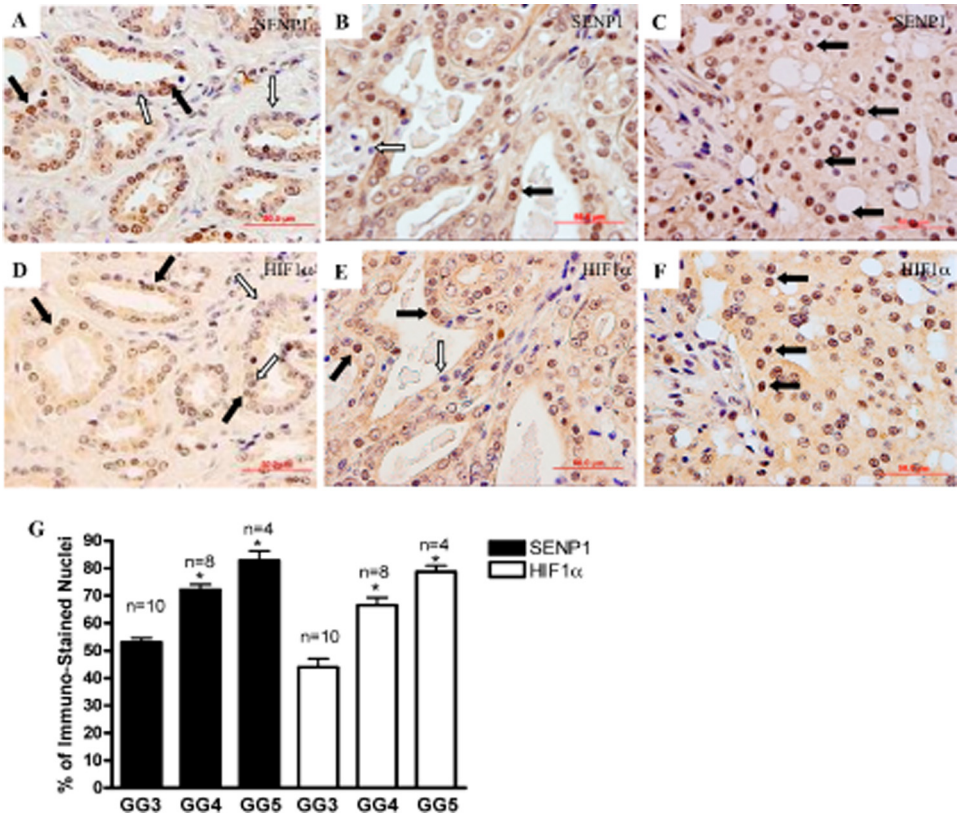

FIGURE 6. **SENP1 levels increase with PCa aggressiveness and correlate with HIF1α levels.** Human prostate tissue samples were obtained following radial prostatectomy and expressed carcinomas with Gleason grades of 3–5. Pre-sectioned samples were assessed for protein expression of SENP1 (*A–C*) and HIF1α (*D–F*) via immunohistochemical analysis. The *black arrows* identify positive staining in the nuclei for the appropriate protein, whereas the *white arrows* illustrate negative nuclear staining. *G*, under ×40 magnification, the total number of nuclei (positive and negative) *versus* the number of positively stained nuclei was determined for a sample that expressed the indicated carcinoma grade. The graph represents the number of positive nuclei observed for either protein with the indicated Gleason grade (*GG*). Student's *t* test was used to evaluate differences in the number of positive nuclei between each Gleason grade for SENP1 and HIF1α, respectively. *, $p < 0.05$.

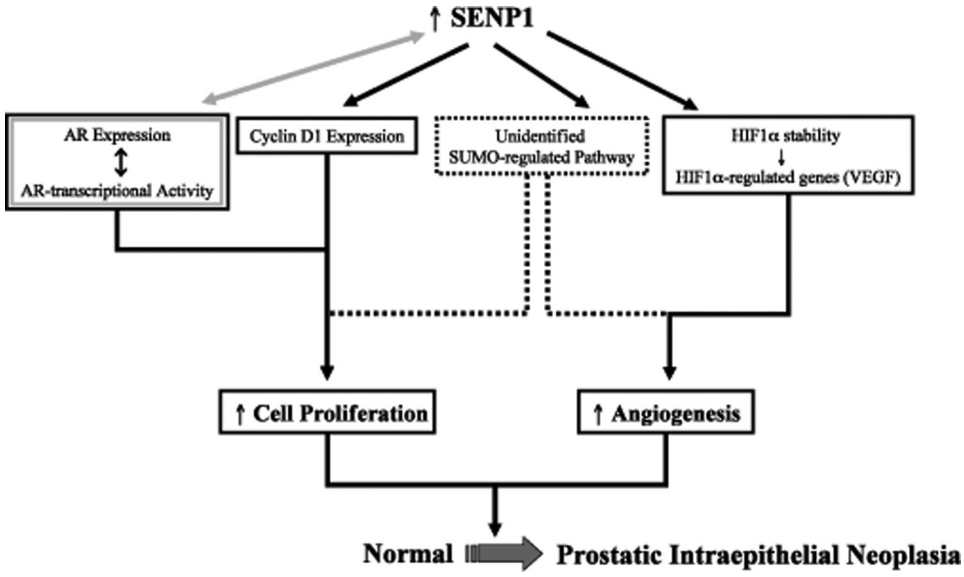

FIGURE 7. **SENP1 induction of prostate pathogenesis.** Shown is a schematic representation of the contribution of SENP1 to the pathogenesis of the prostate gland; a detailed explanation is provided under "Discussion."

oncogenic pathways (9, 10, 12, 17, 18). We have demonstrated that overexpression of SENP1 significantly increases AR-dependent transcription via deconjugation of the AR corepressor HDAC1 (18). More recent data established that an interdependent relationship exists between AR and SENP1, as continuous activation of AR induces induction of *SENP1* gene transcription in LNCaP cells (19). Multiple studies show that AR facilitates transcription of the AR gene; hence, AR is autoregulated (25, 26). To further potentiate the feedback loop, elevated SENP1 levels could enhance AR-dependent transcription and subsequently increase AR expression (illustrated in Fig. 7). The SENP1 transgenic mouse model indicates that, indeed, the up-regulation of SENP1 does promote induction of AR (Fig. 3*D*). An elevation of AR is not normally observed with the onset of human PIN (27, 28), and changes in AR expression have not been reported in other mouse models of PIN. Hence, it is likely that the increase in AR levels is due to elevated SENP1 and not the onset of neoplasia in the transgenic mouse.

A previous report demonstrated that an increase of AR in mouse prostate epithelial cells enhances cell proliferation (20), and our recent results indicated that SENP1 induction mediates AR-induced PCa cell proliferation (19). In this study, we have demonstrated that enhanced cell proliferation is readily observed in the SENP1 transgenic mouse (Fig. 3, *A* and *C*). Although AR would be a major contributor to this augmented cell growth, other factors regulated by SENP1 could also play a part in the induction of cell proliferation. For example, overexpression of SENP1 enhances the key cell cycle regulator cyclin D_1 (Fig. 3*D*) (10), which has been shown to also facilitate PCa cell proliferation (29). AR is known to promote accumulation of cyclin D_1 by increasing protein stability (30); however, because SENP1 overexpression regulates cyclin D_1 gene transcription but not protein stability (supplemental Fig. 2), SENP1 causes cyclin D_1 augmentation via an AR-independent mechanism. Interestingly, several studies have shown that cyclin D_1 accumulation eventually inhibits the activity of AR (31–33). Hence, in the SENP1 transgenic mouse,

it is highly improbable that elevated AR would be solely responsible for the enhanced proliferation and neoplastic lesions because its endogenous inhibitor cyclin D_1 is also up-regulated. Instead, SENP1 simultaneously orchestrates multiple pathways (cyclin D_1, HIF1α, etc.) both dependent and independent of AR to facilitate transformation of the prostate gland (Fig. 7). In addition, SENP1 is ubiquitously expressed throughout the nucleus and efficiently deconjugates numerous other SUMOylated protein substrates (9). Therefore, SENP1 could readily deSUMOylate additional unidentified targets to promote the induction of prostate epithelial cell proliferation and angiogenesis in the SENP1 transgenic mouse model (Fig. 7).

Recently, we showed that SENP1 is essential for HIF1α stability under hypoxic conditions in SENP1-deleted embryos and mouse embryonic fibroblast cells (12). Here, we have demonstrated that overexpression of SENP1 in an adult mouse model significantly enhances expression of nuclear HIF1α. In the well defined PCa mouse model TRAMP, high-grade PIN is accompanied by an increase in HIF1α levels, which is, in turn, required for initiation of the angiogenic switch (34). Our C-line SENP1 transgenic mice exhibit an induction of HIF1α with the initial onset of PIN (or low-grade PIN) at 4 months of age (Fig. 5*A*), suggesting that SENP1 regulation of HIF1α occurs early in prostate pathogenesis. Also, SENP1 overexpression initiates the HIF1α pathways in the prostates of C-line transgenic mice as indicated by the elevation of HIF1α-regulated VEGF. In the TRAMP model, only VEGF mRNA levels are elevated during PIN, with detectable changes in VEGF protein levels in the prostate epithelia only with the emergence of a poorly differentiated carcinoma. In contrast, in our mouse model, we observed significant induction of VEGF protein levels at low-grade PIN (4 months of age) (Fig. 5*F*) and even more dramatic VEGF elevation at 12 months of age (Fig. 5*F*), when the SENP1 transgenic mice concurrently exhibit an increase in microvessel density. Studies have reported that induction of HIF1α, VEGF, and the neovasculature is readily observed in human PIN lesions and therefore is an early event in prostate pathogenesis (15, 16, 23). The onset of angiogenesis in the SENP1 transgenic mouse appears to closely mimic what happens in human prostate carcinogenesis. Because SENP1 levels are enhanced in human PIN, we believe that SENP1 regulates VEGF expression via modulating the nuclear stability of HIF1α and initiates the onset of angiogenesis in human PIN. SENP1 levels also correspond with HIF1α in human PCa (Fig. 6). HIF1α is currently being evaluated as a prognostic marker for PCa aggressiveness. It is intriguing to speculate that because SENP1 modulates HIF1α, SENP1 may be an equally good marker. This fosters the need for more comprehensive studies to evaluate the potential of SENP1 as a prognostic marker in human PCa.

Collectively, our results indicate that a balance between SUMOylation and deSUMOylation is critical for maintaining normal prostate gland physiology. This balance is disturbed with the induction of SENP1 in human PIN and PCa. In this study, we have demonstrated that SENP1 overexpression leads to prostate neoplasia accompanied by an increase in proliferation and angiogenesis, suggesting that the SUMOylation state of targets in the prostate gland closely dictates the growth/oncogenic pathways.

REFERENCES

1. Yeh, E. T., Gong, L., and Kamitani, T. (2000) *Gene* **248,** 1–14
2. Hay, R. T. (2005) *Mol. Cell* **18,** 1–12
3. Geiss-Friedlander, R., and Melchior, F. (2007) *Nat. Rev. Mol. Cell Biol.* **8,** 947–956
4. Mukhopadhyay, D., and Dasso, M. (2007) *Trends Biochem. Sci.* **32,** 286–295
5. Gong, L., Kamitani, T., Fujise, K., Caskey, L. S., and Yeh, E. T. (1997) *J. Biol. Chem.* **272,** 28198–28201
6. Jacques, C., Baris, O., Prunier-Mirebeau, D., Savagner, F., Rodien, P., Rohmer, V., Franc, B., Guyetant, S., Malthiery, Y., and Reynier, P. (2005) *J. Clin. Endocrinol. Metab.* **90,** 2314–2320
7. Lee, J. S., and Thorgeirsson, S. S. (2004) *Gastroenterology* **127,** S51–S55
8. McDoniels-Silvers, A. L., Nimri, C. F., Stoner, G. D., Lubet, R. A., and You, M. (2002) *Clin. Cancer Res.* **8,** 1127–1138
9. Bawa-Khalfe, T., and Yeh, E. T. H. (2010) in *Conjugation and Deconjugation of Ubiquitin Family Modifiers* (Groettrup, M., ed) pp. 170–183, Landes Bioscience and Springer Science+Business Media, Austin, TX
10. Cheng, J., Bawa, T., Lee, P., Gong, L., and Yeh, E. T. (2006) *Neoplasia* **8,** 667–676
11. Montironi, R., Mazzucchelli, R., and Scarpelli, M. (2002) *Ann. N.Y. Acad. Sci.* **963,** 169–184
12. Cheng, J., Kang, X., Zhang, S., and Yeh, E. T. (2007) *Cell* **131,** 584–595
13. Semenza, G. L. (2003) *Annu. Rev. Med.* **54,** 17–28
14. Chan, N., Milosevic, M., and Bristow, R. G. (2007) *Future Oncol.* **3,** 329–341
15. Mazzucchelli, R., Montironi, R., Santinelli, A., Lucarini, G., Pugnaloni, A., and Biagini, G. (2000) *Prostate* **45,** 72–79
16. Pallares, J., Rojo, F., Iriarte, J., Morote, J., Armadans, L. I., and de Torres, I. (2006) *Histol. Histopathol.* **21,** 857–865
17. Cheng, J., Perkins, N. D., and Yeh, E. T. (2005) *J. Biol. Chem.* **280,** 14492–14498
18. Cheng, J., Wang, D., Wang, Z., and Yeh, E. T. (2004) *Mol. Cell. Biol.* **24,** 6021–6028
19. Bawa-Khalfe, T., Cheng, J., Wang, Z., and Yeh, E. T. (2007) *J. Biol. Chem.* **282,** 37341–37349
20. Stanbrough, M., Leav, I., Kwan, P. W., Bubley, G. J., and Balk, S. P. (2001) *Proc. Natl. Acad. Sci. U.S.A.* **98,** 10823–10828
21. Ghafar, M. A., Anastasiadis, A. G., Chen, M. W., Burchardt, M., Olsson, L. E., Xie, H., Benson, M. C., and Buttyan, R. (2003) *Prostate* **54,** 58–67
22. Alqawi, O., Wang, H. P., Espiritu, M., and Singh, G. (2007) *Free Radic. Res.* **41,** 788–797
23. Zhong, H., Semenza, G. L., Simons, J. W., and De Marzo, A. M. (2004) *Cancer Detect. Prev.* **28,** 88–93
24. Lekas, A., Lazaris, A. C., Deliveliotis, C., Chrisofos, M., Zoubouli, C., Lapas, D., Papathomas, T., Fokitis, I., and Nakopoulou, L. (2006) *Anticancer Res.* **26,** 2989–2993
25. Dai, J. L., and Burnstein, K. L. (1996) *Mol. Endocrinol.* **10,** 1582–1594
26. Nelson, P. S., Clegg, N., Arnold, H., Ferguson, C., Bonham, M., White, J., Hood, L., and Lin, B. (2002) *Proc. Natl. Acad. Sci. U.S.A.* **99,** 11890–11895
27. Leav, I., McNeal, J. E., Kwan, P. W., Komminoth, P., and Merk, F. B. (1996) *Prostate* **29,** 137–145
28. Sweat, S. D., Pacelli, A., Bergstralh, E. J., Slezak, J. M., and Bostwick, D. G. (1999) *J. Urol.* **161,** 1229–1232
29. Chen, Y., Martinez, L. A., LaCava, M., Coghlan, L., and Conti, C. J. (1998) *Oncogene* **16,** 1913–1920
30. Xu, Y., Chen, S. Y., Ross, K. N., and Balk, S. P. (2006) *Cancer Res.* **66,** 7783–7792
31. Knudsen, K. E., Cavenee, W. K., and Arden, K. C. (1999) *Cancer Res.* **59,** 2297–2301
32. Petre-Draviam, C. E., Williams, E. B., Burd, C. J., Gladden, A., Moghadam, H., Meller, J., Diehl, J. A., and Knudsen, K. E. (2005) *Oncogene* **24,** 431–444
33. Reutens, A. T., Fu, M., Wang, C., Albanese, C., McPhaul, M. J., Sun, Z., Balk, S. P., Jänne, O. A., Palvimo, J. J., and Pestell, R. G. (2001) *Mol. Endocrinol.* **15,** 797–811
34. Huss, W. J., Hanrahan, C. F., Barrios, R. J., Simons, J. W., and Greenberg, N. M. (2001) *Cancer Res.* **61,** 2736–2743